

# Optical performance characterization of 5 cm aperture size continuous focus tunable liquid crystal lens for resolving Accommodation-Convergence mismatch conflict of AR/VR/3D HMDs

Amit Kumar Bhowmick\*, Afsoon Jamali\*\*, Douglas Bryant\*, Sandro Pintz\*\*, Philip J Bos\*\*

\*Advanced Materials and Liquid Crystal Institute, Kent State University, Ohio, USA

\*\*Meta Reality Labs, Redmond, WA

## Abstract

*Solving the accommodation-convergence mismatch issue, which causes eye fatigue, remains a challenge in the field of AR/VR/3D HMDs. We propose a solution to tackle such vision fatigue by using a large aperture (5 cm) continuous focus tunable liquid crystal lens in addition to fixed power VR lens. To reduce the switching speed to achieve desired optical power swing, our device includes phase resets, similar to a Fresnel lens. Introduction of the phase resets increases response speed significantly, however, also introduces diffraction related issues that is the subject of this paper. In this paper, device demonstration and characterization of a continuous tunable lens with power from 0 D to 1.6 D is shown.*

## Author Keywords

Accommodation-Convergence Conflict, Tunable Lens, Liquid-Crystal lens, Large Aperture Electronic Lens

## 1. Introduction

The accommodation-convergence mismatch issue in near eye displays remain an active challenge in the realm of head mounted display (HMDs).

In the current form of HMDs, the image of the near eye display is focused on a fixed distance which set by the focal length of the fixed VR lens [1]. While wearing the HMDs, the human eye accommodates to that fixed distance. However, the stereoscopic image causes the eyes to converge at a different distance. As a result, the unnatural conflicting accommodation and convergence depth cues creates visual fatigue. [2].

There are several approaches reported so far to solve the problem including light field displays [3], holographic displays [4], volumetric displays [5], multifocal displays [6]. All the reported solutions have their own drawback that ranges from additional bandwidth requirement of the display to compromising the image resolution.

Here, the proposed approach is to use a variable power VR lens system. In addition to fixed power VR lens, the proposed lens system contains a liquid crystal based tunable lens where the focal length of the LC lens can be varied based on users' eye vergence angle [7]. An eye tracker system can be implemented to track eye convergence angle based on the pupil positions. Feedback from the eye tracker can be used to vary optical power of the LC lens so that accommodation and convergence remain on the same plane. While this approach simplifies the need of changing screen resolution or refresh rate, for the application in HMDs, the used LC lens needs to be of high quality, fast, compact and of large aperture. After reviewing all possible technologies, Kramida and Vrishney concluded that liquid crystal lens coupled eye tracker system has the maximum potential to solve the accommodation-convergence mismatch issue of HMDs [8].

The response speed of the liquid crystal is fundamentally limited by the aperture size of the LC lens. Without compromising

switching speed of the lens, recently, we have reported 0 D to 0.80 D optical power swing 5 cm aperture LC lens utilizing a segmented phase profile [9]. Our LC lens is thin, flat, and continuously tunable within designed optical range. However, segmentation of the phase profile introduces diffraction related issues on optical performance of the lens which will depend on the region of the LC lens we are looking at. In this paper, the optical quality characterization of the higher optical power range of 0 D to 1.60 D within the entire lens area by sub dividing into different regions is shown. Optical quality of the LC lens is also investigated by mimicking a VR system.

## 2. Device concept

The LC lens contains concentric ring electrodes connected to inner ring resistor network to obtain parabolic phase profile within lens aperture based on input voltage profile. Using concentric ring electrode structure, very high optical quality, diffraction limited LC lens has been reported for a smaller aperture size (2.4 mm) device [10]. LC lens aperture size greater than 1 cm is challenging in terms of device switching speed, as the achievable optical path difference from a LC cell is limited by the material birefringent value and cell thickness. Optical path difference of a LC cell is linearly proportional to cell thickness, whereas optical path difference of a thin lens is proportional to square of lens radius size. On the other hand, switching speed of LC cell is proportional to square of cell thickness of the cell. Hence, a large aperture LC lens cell requires a large OPD from the LC cell. Relating with switching speed and OPD of LC cell, switching speed of LC lens is proportional to the fourth power of radius of LC lens.

For practical applications, our designed LC lens contains Fresnel like phase resets which reduces the switching time of the device within 500 ms despite being large aperture size of 5 cm (fig. 1). To further increase the switching speed for given optical power of the device, we stack multiple LC lenses. With M number of phase resets and N number of stacked cells, the switching speed of the device reduces by a factor of  $(N \times M)^2$ . The presented 5 cm LC lens has two sub-lenses and has 28 phase resets.

Fig.1 shows the side view of the layer structure and a fabricated LC lens cell. With 28 phase resets, one LC lens cell of thickness 20 micron is capable of tuning optical power between -0.40 D

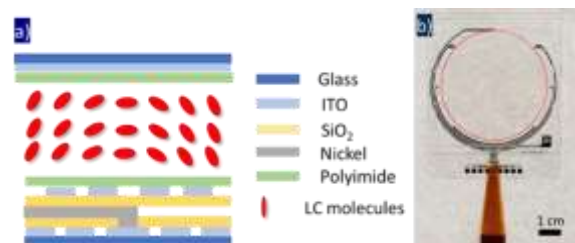


**Fig.1:** a) Side view of inner layer structure of the device, b) fabricated single 5 cm aperture LC lens, red dashed border on the image representing the lens area.

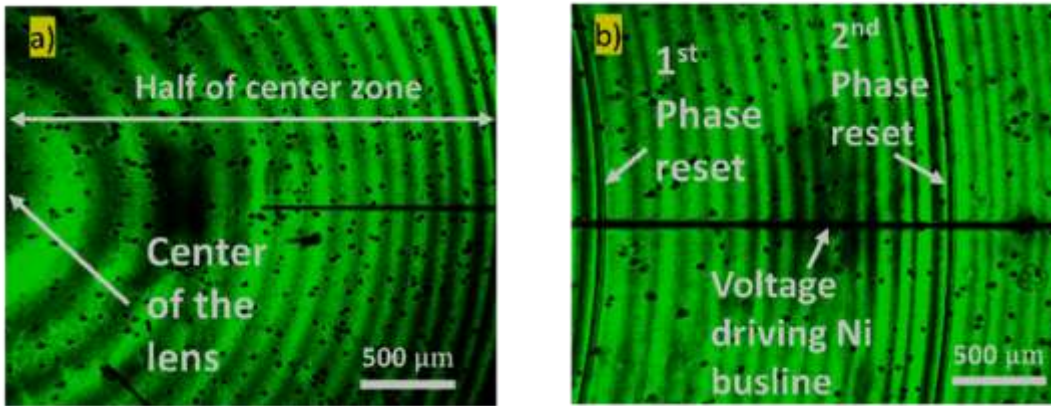


**Fig.2:** Closer look at the phase profile with 543.5 nm wavelength color filter. a) center of the lens where there are no phase resets, b) off-center region of the lens which contains phase resets. The pictures are taken between crossed polarizers to allow visualization of the phase profile. The spacing between the dark lines corresponds to a phase change of a wave of green light.

to +0.40 D. Stacking two cells of equal cell thickness but anti-parallelly rubbed, the continuous tunable power become tunable between optical power -0.80 D to +0.80 D. With a diffraction limited compensator glass lens of fixed power +0.80 D, the tunable optical power range of the LC lens can be made 0 D to 1.60 D. Staking two cells increases tunable optical power range as well as the viewing angle of the device.

As mentioned, the segmented phase profile of the lens, degrades the optical quality. In this lens there are 28 zones of continuous parabolic phase profile, separated by zone boundaries that contain a phase reset. The main source of optical quality degradation is the caused by the zone boundaries. The width of the zone boundaries is the same throughout the cell, but the width of the uniform parabolic phase profile (between the zone boundaries) is large near the center of the lens and becomes less as a function of lens radius. Therefore, the degradation is worse near the edge of the lens and is very low near the center of the lens

While basic design and fabrication details of the discussed device is reported in earlier report[9], in this report, our main goal is given on the characterization of the effect of phase resets and evaluation of the optical quality of the lens at different regions of the lens area where the periodicity of the phase resets varies.

The issue with the phase resets is related to the LC director profile at the phase reset boundary where there is transition from low voltage region to high voltage region. Instead of sharp step wise change of phase at the reset boundary, non-zero width of the of phase reset will cause light scattering into undesirable directions. This scattering can lead to a background haze and a reduction in the MTF of the lens.

Aside from the optical quality degradation due directly to the phase reset, there is the possibility of further degradation when phase profile change at the boundary of two zones is not an integer number of wavelengths. However, through careful calibration of the device, this can be minimized.

### 3. Characterization of the phase profile

In our LC lens, we have used a positive birefringence ( $\Delta n = n_e - n_o > 0$ ) LC material, as a result, with the application of electric field, the director of the material tends to orient in the direction of applied field. The goal of voltage tuning is to achieve parabolic phase profile within each zone, as well as keep phase step at the reset boundary to be an integer multiple of wavelengths of light near the center of the visible spectrum. As human eye is most sensitive to

green light, we use color filter of wavelength  $\lambda = 543.5$  nm to tune the voltage profile.

As the voltage vs phase response of the LC material is not linear, our device implements eight voltage inputs instead of one. With eight voltage inputs, linear relationship between voltage and phase can be obtained between two input voltages as a result of each ring electrode being connected by an inter-ring resistor

Figure 2 shows microscopic images of two regions of a LC lens tuned to be +0.80D. There is no discontinuity of phase profile at the center of the LC lens within 1<sup>st</sup> zone, hence, diffraction related performance is independent on wavelength of light. In case of off-center lens area, the phase profile contains phase resets.

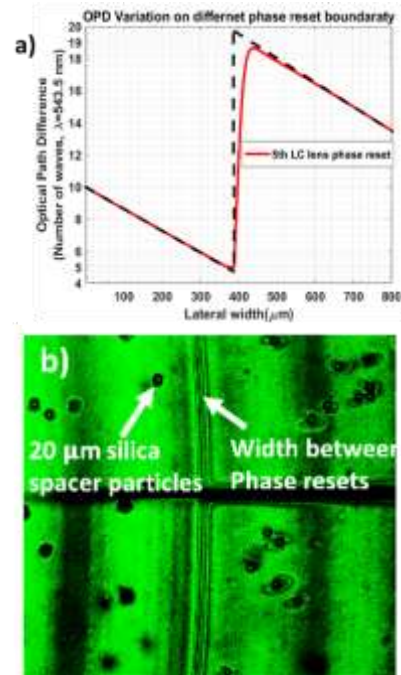


**Fig. 3** a) Simulated phase resets of the LC lens (red) compared to ideal Fresnel reset (black dashed line), b) closer look at the phase profile to show width of phase distortion correlates with cell spacer thickness.

From a fabricated device of cell thickness of 20- micron, the width of the zone boundary, which causes phase distortion, is

found to be 20- microns (fig. 3(b)). This result agrees with the calculated phase reset with as shown in fig 3(a).

#### 4. Image performance evaluation

Image performance of the lens is evaluated with negative chrome USAF 1951 test target back-illuminated with fluorescent light. The image formed by the LC lens at power on/off condition is captured by Canon EOS Rebel XSi/450D equipped with 100 mm macro lens. DSLR camera lens has focus ring which can be adjusted when image become defocus while LC lens optical power is changed.

As optical performance of the device is dependent on area of the lens as phase resets periodicity is reducing along with the radius of the lens. Taking into consideration the human eye average pupil size of 5 mm, we divide the entire lens aperture into five sub apertures of equal width of 5 mm. Center of these five sub apertures are 0 mm, 2.5 mm, 7.5 mm, 12.5 mm, 17.5 mm away from the center of entire lens, respectively. Considering distance between LC lens and human eye as 2 cm, center of sub apertures correlates with gaze angle  $0^\circ$ ,  $14^\circ$ ,  $27^\circ$ ,  $37^\circ$ ,  $45^\circ$ , respectively.

The center sub aperture does not contain phase resets within aperture width. Only the effect of electrode gaps can degrade image quality. As the fabricated cell contain floating electrodes, the effect of electrode gap is minimized, and diffraction limited optical performance is observed. In the case of fig 4(a) LC lens is powered off and DSLR camera lens focus ring is adjusted to find best focus. When LC lens is powered on at  $+0.80$  D at fig 4(b), the image become defocused due to focal length change caused by LC lens.

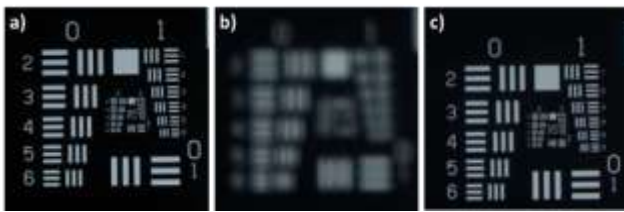


**Fig. 4:** Optical quality of the LC lens at the center of the lens, a) LC lens off, b) LC lens on at  $+0.80$  D, c) LC lens on at  $+0.80$  D while DSLR camera lens focus is readjusted to focus the defocused image of case (b).

In fig 4(c), DSLR camera is readjusted to make sharp focus of the image while LC lens power is  $+0.80$  D.

Image quality of other sub apertures, towards the edge, is degraded by the phase resets. Going from inner lens region towards to outer lens region, phase resets periodicity is decreasing. Hence, outer sub apertures will contain a higher density of phase resets, respectively. With increasing phase reset densities in the sub apertures, continuous degradation of the image quality is observed. In fig. 5, we have shown zoomed picture of group 0 element 6 of the air force chart at all sub aperture positions to compare the image quality based on lens radius. A 5 mm aperture stop is used whose position is changed laterally according to the sub apertures positions to capture pictures of the fig. 5. Hence, only on-axis light propagation performance is evaluated in this case.

Images shown in fig. 5 are taken when distance between air force chart target and LC lens is 320 mm. Resolution of group 0 element 6 of air force chart corresponds to  $1.78$  lp/mm. Multiplying the distance between target and LC lens, spatial resolution  $1.78$  lp/mm corresponds to  $10$  cyc/deg. MTF is measured at  $10$  cyc/deg by taking intensity modulation around the group element along the yellow line. MTF measured at  $+0.80$  D at different viewing angle are measured and compared with simulated MTF value (fig.6). Simulation results are calculated by using a numerical director field

calculation based on the Frank free energy and the geometry of the fabricated device.

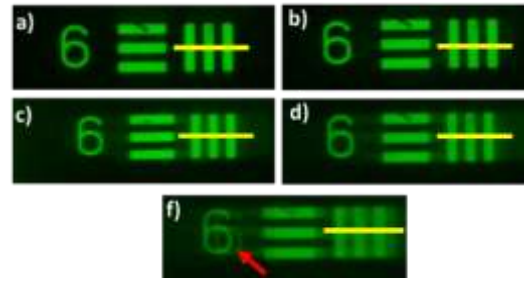


**Fig. 5:** Optical performances of the LC lens based on different sub aperture positions of the LC lens tuned to be  $+0.80$ D in the presence of green filter ( $\lambda=543.5$  nm). Subfigures a), b), c), d), e), are with the camera looking through the sub apertures, where the center of each sub aperture corresponds to gaze angle of  $0^\circ$ ,  $14^\circ$ ,  $27^\circ$ ,  $37^\circ$ , and  $45^\circ$ , respectively.

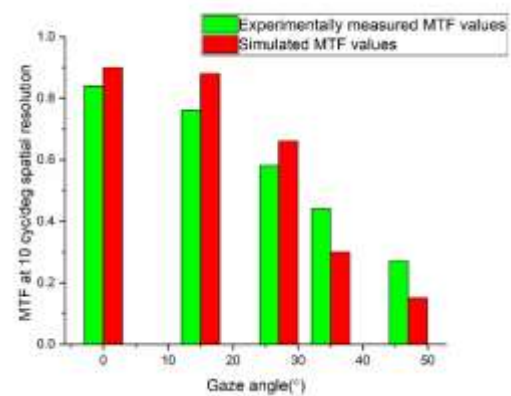


**Fig. 6:** Comparison of experimentally measured MTF and calculated MTF at  $10$  cyc/deg spatial resolution at LC power  $+0.80$  D

While a diffracted image (indicated by red arrow in fig. 5) is seen in case of  $45$ -degrees gaze angle, other sub apertures show indication of haze in the picture instead of diffracted image. Scattering of light from to the width of phase reset boundary can explain the origin of haze. As going outward, the phase reset densities are increasing, scattering effect also increasing

#### 5. Demonstration on lab-based VR system

In this section, a device performance evaluation by mimicking traditional VR system is shown. Instead of head mounted display and a strong magnifying lens (that can degrade the image quality), we have used a large screen size LCD monitor screen which kept close distance to the lens system to provide wide field of view. The lens system contains a fixed power glass lens along with LC lens which is a stack of two anti-parallelly rubbed liquid crystal lens cells. While each lens cell can be tuned continuously from  $-0.40$  D to  $+0.40$  D, for the purpose of demonstrating we have used maximum optical power of each lens cell. Hence, with optical power of  $+0.40$  D on each cell, the power of LC lens stack is  $+0.80$  D. By changing the voltage profile of LC lens, the optical power can be switched to  $-0.80$  D, with an additional compensator lens of fixed power  $+0.80$  D, the discussed lens system is capable of tunable range from  $0$  D to  $1.60$  D. Considering the compensator lens as diffraction-limited, the optical quality test of LC lens at  $+0.80$ D also corresponds to optical quality at  $1.60$  D.

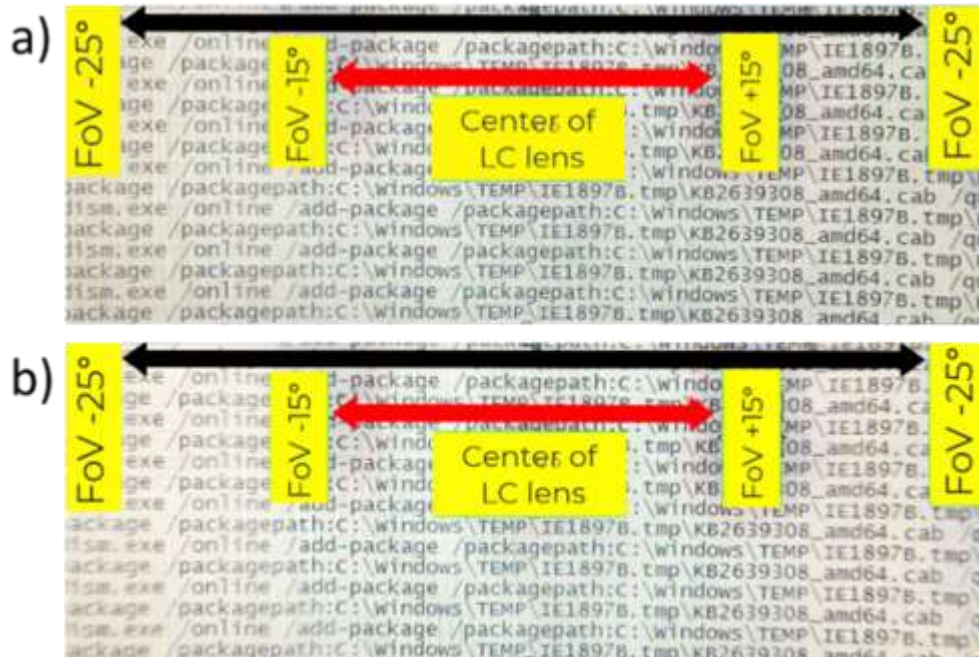


**Fig. 7:** Optical quality evaluation images on a lab-based VR system, a) LC lens is off for case-1, b) LC lens at +0.80 D for on axis view with +/- 25 degrees gaze angle. (note: the camera is refocused as the lens power changes)

The image of the displayed picture is captured with a phone camera whose aperture size is comparable to human eye aperture size. For evaluation, we have chosen a black text on a white background. From the distance of the phone camera, width of each letter on the displayed image is about 2.5 mm. Distance between display and lens systems is 17 cm, the distance between center of the phone camera lens and lens system is 1.8 cm.

Figure 7 shows the image taken by the phone camera looking straight through the center of LC lens which cover FoV that cover gaze angle +/- 28 degrees. Subfigure (a) is with the LC lens unpowered, and subfigure (b) is with the LC lens powered to be +0.8D.

## 6. Conclusion

In this report, we have shown the characterization of the large aperture LC lens within entire viewing region by sub dividing into different aperture regions. From the characterization, possibly acceptable MTF values are recorded within a gaze angle of about 30 degrees. The Image quality degrades towards the outer edge of the lens due to scattering of light and diffraction issues related to segmented phase resets. However, the user wearing HMDs is expected to move their head to view images more than 25 degrees off axis. Therefore, the degradation of the image quality will only be in large FOV angles where the retina has lowered resolution and may be unnoticeable.

## 7. Acknowledgement

This project is funded by Meta Reality Labs.

## 8. Reference

1. Shibata, T., et al., *Stereoscopic 3-D display with optical correction for the reduction of the discrepancy between accommodation and convergence*. Journal of the Society for Information Display, 2005. **13**(8): p. 665-665.
2. Mon-Williams, M., J.P. Warm, and S. Rushton, *Binocular vision in a virtual world: visual deficits following the wearing of a head-mounted display*. Ophthalmic and Physiological Optics, 1993. **13**(4): p. 387-391.
3. Lanman, D. and D. Luebke, *Near-eye light field displays*. ACM Transactions on Graphics, 2013. **32**(6): p. 1-10.
4. Maimone, A., A. Georgiou, and J.S. Kollin. *Holographic near-eye displays for virtual and augmented reality*. Association for Computing Machinery.
5. Love, G.D., et al., *High-speed switchable lens enables the development of a volumetric stereoscopic display*. Optics Express, 2009. **17**(18): p. 15716-15716.
6. Akeley, K., et al., *A stereo display prototype with multiple focal distances*. ACM Trans. Graph., 2004. **23**(3): p. 804-813.
7. Jamali, A., et al., *LC lens systems to solve accommodation/convergence conflict in three-dimensional and virtual reality displays*. Optical Engineering, 2018. **57**(10): p. 1-1.
8. Kramida, G., *Resolving the vergence-accommodation conflict in head-mounted displays*. IEEE Transactions on Visualization and Computer Graphics, 2016. **22**(7): p. 1912-1931.
9. Bhowmick, A.K., et al., *31-5: Student Paper: Liquid Crystal Based 5 cm Adaptive Focus Lens to Solve Accommodation-Convergence (AC) Mismatch Issue of AR/VR/3D Displays*. SID Symposium Digest of Technical Papers, 2021. **52**(1): p. 410-413.
10. Li, L., D. Bryant, and P.J. Bos, *Liquid crystal lens with concentric electrodes and inter-electrode resistors*. Liquid Crystals Reviews, 2014. **2**(2): p. 130-154.
11. Jamali, A., et al., *Design of a large aperture tunable refractive Fresnel liquid crystal lens*. Applied Optics, 2018. **57**(7): p. B10-B10.
12. Jamali, A., et al., *Large area liquid crystal lenses for correction of presbyopia*. 2020.